

THREE-DIMENSIONAL MAGNETOHYDRODYNAMIC SIMULATIONS OF ACCRETION TO AN INCLINED ROTATOR: THE “CUBED SPHERE” METHOD

A. V. KOLDOBA,¹ M. M. ROMANOVA,² G. V. USTYUGOVA,³ AND R. V. E. LOVELACE²

Received 2002 March 12; accepted 2002 July 11; published 2002 August 5

ABSTRACT

We describe a three-dimensional, Godunov-type numerical magnetohydrodynamics (MHD) method designed for studying disk accretion to a rotating magnetized star in the general case where the star’s rotation axis, its magnetic moment, and the normal to the disk all have different directions. The equations of ideal MHD are written in a reference frame rotating with the star, with the z -axis aligned with the star’s rotation axis. The numerical method uses a “cubed sphere” coordinate system that has advantages of Cartesian and spherical coordinate systems but does not have the singular axis of the spherical system. The grid is formed by a sequence of concentric spheres of radii $R_j \propto q^j$, with $j = 1, \dots, N_R$ and $q = \text{constant} > 1$. The grid on the surface of the sphere consists of six sectors, with the grid on each sector topologically equivalent to the equidistant grid on the face of a cube. The magnetic field is written as a dipole component plus deviations, and only the deviations are calculated. Simulation results are discussed for the funnel flows to a star with dipole moment μ at an angle $\Theta = 30^\circ$ to the star’s rotation axis Ω , which is aligned with the normal to the disk. Results are given for different grids ($N_R \times N^2$) from 26×15^2 (coarsest) to 50×29^2 (finest). We observe that the qualitative features of the accretion flows are very similar for the different grids, but the coarser grid is affected by numerical viscosity. We compare our three-dimensional results for $\Theta = 0$ with the axisymmetric (two-dimensional), spherical coordinate system simulations of funnel flows of Romanova et al. Two important new three-dimensional features are found in these simulations: (1) The funnel flow to the stellar surface is mainly in two streams that approach the star from opposite directions. (2) In the x - z cross section of the flow containing μ and Ω , the funnel flow often takes the longer of the two possible paths along magnetic field lines to the surface of the star. A subsequent paper will give a detailed description of the method and results on three-dimensional funnel flows at different inclination angles Θ .

Subject headings: accretion, accretion disks — magnetic fields — MHD — stars: formation — stars: magnetic fields — stars: neutron

1. INTRODUCTION

There are many X-ray binary systems consisting of a rotating neutron star with a dipole magnetic field that accretes matter from the other star. Commonly, the accreting matter forms a disk as it approaches the neutron star. The neutron star’s magnetic dipole axis μ is not aligned with its rotation axis Ω in the observed pulsating sources. Furthermore, in general μ and Ω are not aligned with the normal to the disk. That is, the dipole moment is inclined relative to the disk. In some systems, such as Her X-1, this inclination is evident from the observations (e.g., Trümper et al. 1986). Models of magnetohydrodynamic (MHD) disk accretion to a rotating star with an aligned dipole magnetic field have been discussed by a number of authors (e.g., Ghosh & Lamb 1979; Camenzind 1990; Königl 1991; Lovelace, Romanova, & Bisnovatyi-Kogan 1995, 1999; Ostriker & Shu 1995; Li & Wilson 1999; Koldoba et al. 2002). Analytical investigations of three-dimensional accretion to an inclined magnetic rotator were done by Arons & Lea (1976a, 1976b), Lipunov (1978a, 1978b), Sharlemann (1978), Aly (1980), Lai (1999), and Terquem & Papaloizou (2000). However, the essential aspects of this problem are three-dimensional and are not amenable to an analytic approach.

In this Letter we describe a method developed specifically for studying MHD accretion to nonaligned magnetic rotators.

The method is based on the “cubed sphere” coordinate system proposed by Sadourny (1972) and discussed by Ronchi, Iacono, & Paolucci (1996). We solve the equations of ideal MHD in a reference frame rotating with the star using cubed sphere coordinates and a Godunov-type method. In contrast with Ronchi et al. (1996), our simulations are in three dimensions rather than on the surface of the sphere, and furthermore we solve the equations of MHD.

An important question is what grid resolutions are necessary for obtaining valid results for the problem of MHD disk accretion to a rotating star with magnetic moment misaligned with the star’s rotation axis? Because three-dimensional MHD simulations are very time consuming, it is important to find an optimal grid resolution. Here we discuss results from simulations for the case where the star’s magnetic moment is inclined at an angle $\Theta = 30^\circ$ to the star’s rotation axis, which is aligned with the normal to the disk. In § 2 we describe our simulation methods. In § 3 we summarize results of our three-dimensional simulations of funnel flows to a rotating misaligned dipole and compare three-dimensional simulation results for an aligned dipole with our earlier axisymmetric simulation results (Romanova et al. 2002). Conclusions of this work are given in § 4.

2. SIMULATION METHOD

We consider a rotating magnetized star surrounded by an accretion disk and its corona. This problem is difficult to treat numerically because the magnetic field varies strongly with distance from the star ($\sim 1/R^3$), and it is rapidly varying in the laboratory inertial reference frame. To minimize errors in calculating the magnetic force, the magnetic field \mathbf{B} is decomposed

¹ Institute of Mathematical Modeling, Russian Academy of Sciences, Moscow 125047, Russia; koldoba@spp.keldysh.ru.

² Department of Astronomy, Cornell University, 410 Space Science Building, Ithaca, NY 14853-6801; romanova@astro.cornell.edu, RVL1@cornell.edu.

³ Keldysh Institute of Applied Mathematics, Russian Academy of Sciences, Moscow 125047, Russia; ustyugg@spp.keldysh.ru.

into the “main” dipole component of the star, \mathbf{B}_0 , and the component, \mathbf{B}_1 , induced by currents in the disk and in the corona. Because $\nabla \times \mathbf{B}_0 = 0$, the magnetic force is $(\mathbf{J} \times \mathbf{B})/c = (\nabla \times \mathbf{B}_1) \times (\mathbf{B}_0 + \mathbf{B}_1)/4\pi$, which does not involve the terms $O(\mathbf{B}_0^2)$ (Tanaka 1994; Powell et al. 1999).

Another difficulty in this problem is that the dipole moment changes with time. It rotates with angular velocity Ω so that the “main” field \mathbf{B}_0 also changes with time. Consequently, in the induction equation there is a large term involving \mathbf{B}_0 . To overcome this difficulty we use a coordinate system rotating with angular velocity Ω , in which the magnetic moment of the star μ and the “main” field \mathbf{B}_0 do not depend on time.

2.1. MHD Equations in the Rotating Frame

Let Ω be the angular velocity of rotation of the star. In the laboratory (inertial) reference frame, the MHD equations are $D\rho/Dt + \rho\nabla \cdot \mathbf{u} = 0$, $\rho D\mathbf{u}/Dt = -\nabla p + (\nabla \times \mathbf{B}) \times \mathbf{B}/4\pi + \rho\mathbf{g}$, $DS/Dt = 0$, and $D\mathbf{B}/Dt = (\mathbf{B} \cdot \nabla)\mathbf{u} - \mathbf{B}(\nabla \cdot \mathbf{u})$. Here \mathbf{u} is the bulk velocity of the plasma, S the specific entropy, \mathbf{B} the magnetic field, and $D/Dt = \partial/\partial t + \mathbf{u} \cdot \nabla$ the convective derivative in the inertial frame.

The relations between the variables in the inertial frame and the reference frame rotating at rate Ω for a given fluid particle are $\mathbf{u} = \mathbf{v} + \Omega \times \mathbf{R}$, $\mathbf{B} = \mathbf{B}$, where \mathbf{v} is velocity of plasma in the rotating frame. The convective derivatives of scalar variables f do not change: $Df/Dt = df/dt$, where $d/dt = \partial/\partial t + (\mathbf{v} \cdot \nabla)$ is the convective derivative in the rotating frame. However, convective derivatives of vector variables transform as follows: $D\mathbf{F}/Dt = d\mathbf{F}/dt + \Omega \times \mathbf{F}$.

Because $\nabla \cdot (\Omega \times \mathbf{R}) = 0$, the continuity equation is $d\rho/dt + \rho\nabla \cdot \mathbf{v} = 0$. In the Euler equation in the rotating frame, there are two inertial terms added to the right-hand side, the Coriolis force and the centrifugal force, $\rho d\mathbf{v}/dt = -\nabla p + (\nabla \times \mathbf{B}) \times \mathbf{B}/4\pi + \rho\mathbf{g} + 2\rho\mathbf{v} \times \Omega - \rho\Omega \times (\Omega \times \mathbf{R})$. In the induction equation, $(\mathbf{B} \cdot \nabla)\mathbf{u} = (\mathbf{B} \cdot \nabla)\mathbf{v} + (\mathbf{B} \cdot \nabla)(\Omega \times \mathbf{R}) = (\mathbf{B} \cdot \nabla)\mathbf{v} + \Omega \times \mathbf{B}$. Therefore, in the rotating reference frame the induction equation has the same form, $d\mathbf{B}/dt = (\mathbf{B} \cdot \nabla)\mathbf{v} - \mathbf{B}(\nabla \cdot \mathbf{v})$.

Putting the equations in Eulerian form in the rotating frame, one finds that the new terms are the Coriolis and centrifugal forces in the Euler equation. The full set of equations is $\partial\rho/\partial t + \nabla \cdot (\rho\mathbf{v}) = 0$, $\partial(\rho\mathbf{v})/\partial t + \nabla \cdot \mathbf{T} = \rho\mathbf{g} + 2\rho\mathbf{v} \times \Omega - \rho\Omega \times (\Omega \times \mathbf{R})$, $\partial(\rho S)/\partial t + \nabla \cdot (\rho S\mathbf{v}) = 0$, and $\partial\mathbf{B}/\partial t = \nabla \times (\mathbf{v} \times \mathbf{B})$, where \mathbf{T} is the stress tensor with components $T_{ik} \equiv p\delta_{ik} + \rho v_i v_k + (B^2\delta_{ik}/2 - B_i B_k)/4\pi$. We do not include shocks in the present work as implied by the entropy conservation equation.

2.2. The Grid

As shown in Figure 1, the three-dimensional grid consists of a set of concentric spheres of radii R_j , with $j = 1, \dots, N_R$. The distribution of R_j is chosen to be inhomogeneous with $R_j = R_* q^{j-1}$, where q is constant and R_* is the radius of the numerical star. This choice implies $\Delta R_j/R_j = q - 1$. The grid on the surface of the sphere consists of six sectors, with the grid on each sector topologically equivalent to the equidistant grid on the face of a cube. In each sector, the grid of $N \times N$ cells is formed by the arcs of great circles separated by equal angles. For example, the $+x$ sector is formed by the arcs of great circles going through the y - and z -axes.

This three-dimensional grid gives high spatial resolution close to the star, which is important to our study of accretion to a rotating star with dipole magnetic field. Because $\Delta R_j/R_j =$

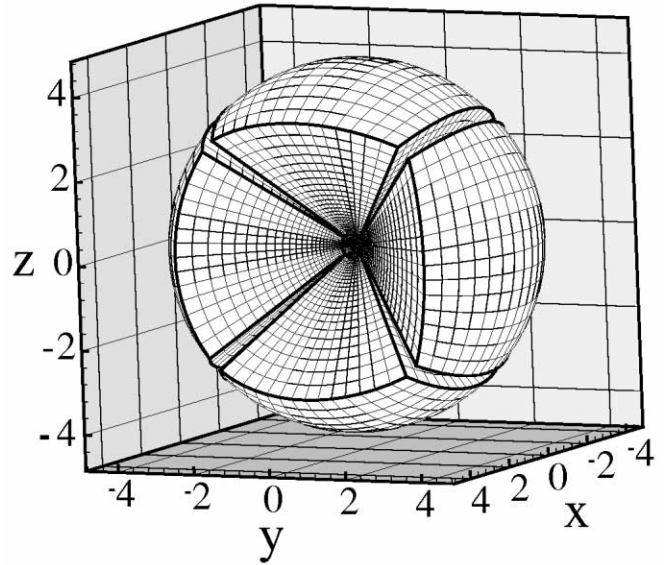


FIG. 1.—Cubed sphere grid, which consists of six sectors. The $+x$ sector is omitted in order to show the inner structure of the grid. Grid is inhomogeneous in the R -direction in such a way that the cells are roughly cubical independent of R .

constant, the shape of the volume elements is approximately cubical independent of R .

The present study uses the scalings introduced by Romanova et al. (2002), where the initial inner radius of the disk and the beginning of the funnel flow (in the aligned, axisymmetric case) are at a radial distance R_0 . Distances are measured in units of R_0 , velocities in units of $v_0 \equiv (GM/R_0)^{1/2}$, and time in units of $P_0 \equiv 2\pi R_0/v_0$. With B_0 the magnetic field at the surface of the star, we can define a reference density as $\rho_0 \equiv B_0^2/v_0^2$ and a reference value for the magnetic moment as $\mu_0 \equiv B_0 r_0^3$. In this study, the dimensionless radius of the numerical star is $R_{\min}/R_0 = 0.35$, and the outer radius of the simulation volume is $R_{\max}/R_0 \approx 4.8$. We present results for two cubed sphere grids, one with $N_R \times N^2 = 50 \times 29^2$ cells in each of the six sectors (a total of $\approx 2.5 \times 10^5$ cells) and the other with 26×15^2 cells per sector (a total of $\approx 3.5 \times 10^4$ cells). For the first case $q = 1.055$, while for the lower resolution case $q = 1.11$.

2.3. Boundary Conditions

At the inner boundary $R = R_{\min}$ (the “numerical star”), we assume “free” boundary conditions $\partial/\partial R = 0$ for all variables. This boundary condition corresponds to absorption of incoming matter so that there is no standoff shock. This boundary is treated as a rotating perfect conductor $\Omega = \Omega\hat{z}$. The flow velocity \mathbf{v} was corrected in such a way that in the reference frame rotating with the star it is parallel to \mathbf{B} at $R = R_{\min}$, that is, $\mathbf{B} \times \mathbf{v} = 0$ at R_{\min} . The boundary condition at R_{\min} on the magnetic field has $\partial(RB_\phi)/\partial R = 0$. At the outer boundary $R = R_{\max}$, free boundary conditions are taken for all variables.

2.4. Initial Conditions

A star of mass M is located at the origin of the coordinate system. The initial magnetic field is the tilted dipole field of the star, $\mathbf{B}_0 = 3(\mu \cdot \mathbf{R})\mathbf{R}/R^5 - \mu/R^3$, where μ is tilted by an angle Θ from the z -axis (which is $\|\Omega$). As initial conditions, we set up a low-temperature (T_d), high-density (ρ_d) disk with

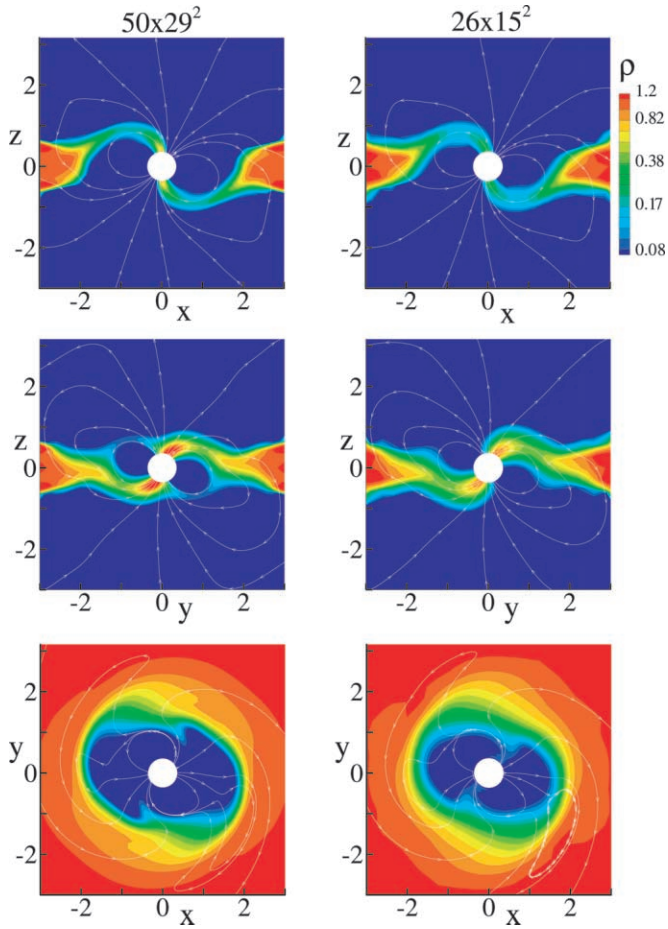


FIG. 2.—Results of three-dimensional MHD simulations of disk accretion to a rotating star with magnetic moment μ tilted $\Theta = 30^\circ$ to the rotation axis Ω . Two grids are shown, $N_R \times N^2 = 50 \times 29^2$ (left-hand panels) and 26×15^2 (right-hand panels) after $t = 1.5P_0$, where P_0 is the period of rotation of the disk at R_0 . Shading or color represents the density, while the lines are magnetic field lines. The x - z cross section is the plane containing Ω and μ . The (x, y) -plane is the midplane of the disk at large distances from the star. Note that N_R is the number of grid cells in the radial direction, while $N \times N$ is the number of cells on the surfaces of each of the six sectors of the cubed sphere.

a high-temperature ($T_c \gg T_d$), low-density ($\rho_c \ll \rho_d$) corona filling the remainder of the simulation region. The disk rotates with the same axis as the rotation of the star with angular velocity close to the Keplerian value $\omega \approx \Omega_K$. The disk extends inward to a radius R_0 as discussed by Romanova et al. (2002) for the case of an aligned rotator. At this distance, the ram pressure of the disk matter is on the order of the magnetic pressure of the dipole, $p + \rho v^2 = B^2/8\pi$. Initially, at any cylindrical radius r from the rotation axis, we rotate the corona and the disk at the same angular rate. This avoids a jump discontinuity of the angular velocity of the plasma at the boundary between the disk and the corona. Of course this distribution of ω in the corona leads to twisting of the dipole magnetic field lines. However, the twisting is smoothly distributed along the magnetic field lines, and it does not lead to fast evolution of the disk-corona system.

2.5. Godunov-type Finite-difference Scheme

All variables are evaluated at the centers of the cells. All vector variables are expressed in terms of their Cartesian components. Finite-difference equations are written for Cartesian

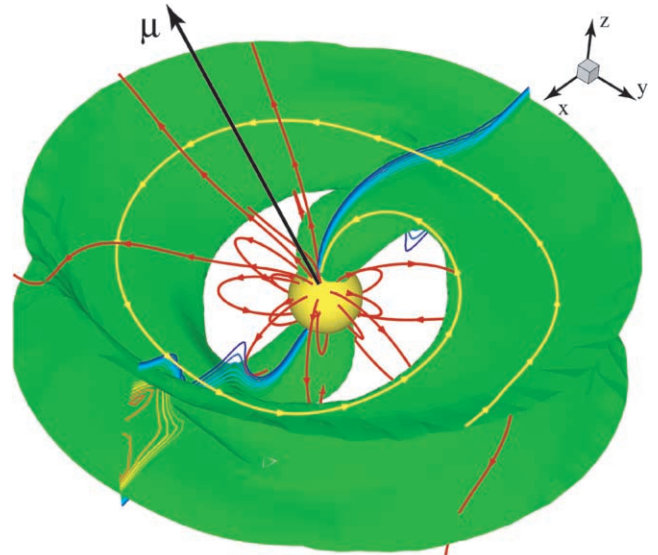


FIG. 3.—Three-dimensional view of the funnel flow to a rotating star with Ω parallel to the z -axis and with the dipole moment μ tilted $\Theta = 30^\circ$ away from the z -axis in the (x, z) -plane. The grid was $N_R \times N^2 = 50 \times 29^2$, and the flow is shown at $t = 2.5P_0$, where P_0 is the period of rotation of the disk at R_0 . Thick arrow represents the star's magnetic moment. Red lines represent magnetic field lines. Yellow spiral line is a streamline. Nested blue and yellow lines are isodensity lines in the (x, z) -plane. Central sphere represents the star, which has a radius $R_* = 0.35R_0$. The funnel flow close to the star is seen to be in two streams that approach the star from opposite directions. Density of the green surface shown is $0.35\rho_0$, where ρ_0 is defined in § 2.2.

components of vector variables. The finite-difference scheme of Godunov's type has the form

$$\frac{U^{p+1} - U^p}{\Delta t} V + \sum_{m=1, \dots, 6} s_m \mathcal{F}_m = Q. \quad (1)$$

Here $U = \{\rho, \rho \mathbf{v}, \mathbf{B}, \rho S\}$ is the “vector” of densities of conserved variables, \mathcal{F}_m is the “vector” of flux densities normal to the face “ m ” of the cell, s_m is the area of the face m , V is the volume of the cell, Q is the intensity of sources in the cell, and Δt is the time step.

To calculate the flux densities \mathcal{F}_m , an approximate Riemann solver is used, namely, an eight-wave Roe-type approximate Riemann solver analogous to one described by Powell et al. (1999). The \mathcal{F} -values are represented as

$$\mathcal{F}_m = \frac{1}{2} (\mathcal{F}' + \mathcal{F}'') - \frac{1}{2} \sum_a v_a |\lambda_a| A_a \mathcal{R}_a. \quad (2)$$

Here \mathcal{F}' and \mathcal{F}'' are flux densities normal to the face m of the cell coming from neighboring cells and v_a are numerical coefficients that regulate the accuracy of the method. These are calculated using values of variables in the cells that are separated by this face; λ_a represents the velocities of the waves in the direction of the normal to the face, A_a the wave amplitudes, and \mathcal{R}_a the right-hand eigenvectors for the eight types of waves, $a = (E, B, \pm A, \pm F, \pm S)$ (see, e.g., Brio & Wu 1984; Powell et al. 1999).

As a test of our three-dimensional code, spherical Bondi accretion (Bondi 1952) was simulated for the case of a magnetic

monopole field, $\mathbf{B} \propto 1/R^2$, with a grid of 50×11^2 in each sector. The simulations show good agreement with the radial dependence of the Bondi solution and with the predicted accretion rate.

3. SIMULATIONS OF FUNNEL FLOWS

Here we discuss simulation results for the case where the star's magnetic moment is inclined at an angle $\Theta = 30^\circ$ to the rotation axis $\mathbf{\Omega}$, which is parallel to the normal of the disk. The magnetic moment of the star and the density of the disk are such that the ram pressure of the disk is approximately equal to the magnetic pressure of the dipole at the inner radius of the disk R_0 at $t = 0$. Thus, the funnel flow is expected to start from about this radius, as observed in our axisymmetric simulations (Romanova et al. 2002). We rotate the star with angular velocity $\Omega_* = g(GM/R_0^3)^{1/2}$, where $g = 0.19$. The corotation radius of the star r_{cor} is the distance where the centrifugal force $\Omega_*^2 r$ equals the gravitational force GM/r^2 ; that is, $r_{\text{cor}} = (GM/\Omega_*^2)^{1/3}$. It follows that $r_{\text{cor}} = R_0/g^{2/3} \approx 3R_0$.

Some information about the three-dimensional MHD flow can be obtained from the three orthogonal slices, an (x, z) slice at $y = 0$, a (y, z) slice at $x = 0$, and an (x, y) slice at $z = 0$. Figure 2 shows these cross sections for different grids. The most refined grid used in the present simulations has $N_R \times N^2 = 50 \times 29^2$ cells in each of the six sectors of the cubed sphere. The coarsest grid has 26×15^2 cells in each sector. Linking with a spherical coordinate system (R, θ, ϕ) , we have the correspondence for the number of cells, $N_R \times N_\theta \times N_\phi = 6N_R \times N^2$. We observed that the slices of the accretion flows are closely similar for the different grids. Namely, with decreasing distance, the disk ends and matter starts to flow out of the plane of the disk into the funnel flow at radii $R \approx 2R_0$ in the x -direction and at $R \approx 1.7R_0$ in the y -direction. In the (x, z) slice (which is the plane

containing μ and $\mathbf{\Omega}$), the funnel flow takes the longer of the two paths along the magnetic field. This we find to be a distinctive effect of the three-dimensional accretion flow to a misaligned dipole. Figure 3 shows a three-dimensional view of the funnel flow. Close to the star, the flow is in two streams that approach the star from opposite sides.

As a test of our code, we did three-dimensional simulations of accretion to an aligned rotator ($\mu \parallel \mathbf{\Omega}$) and analogous two-dimensional axisymmetric simulations in spherical coordinates with the number of cells in the meridional plane $N_R \times N_\theta = 50 \times 29$. Results of the two- and three-dimensional simulations show qualitatively similar funnel flows at the same elapsed times.

4. CONCLUSIONS

We developed a new three-dimensional MHD simulation code for studying the accretion flows to rotating stars with misaligned dipole magnetic fields. New three-dimensional features are found in the simulations of disk accretion to a rotating star with dipole moment μ inclined by an angle Θ to the star's rotation axis. Specifically, in the x - z cross section of the flow containing μ and $\mathbf{\Omega}$, the funnel flow takes the longer of the two possible paths along magnetic field lines to the surface of the star. Furthermore, the funnel flow to the stellar surface is mainly in two streams that approach the star from opposite directions. A subsequent paper will give a detailed analysis of the funnel flows at different inclination angles Θ .

This work was supported in part by NASA grants NAG 5-9047 and NAG 5-9735 and by NSF grant AST 99-86936. M. M. R. is grateful to an NSF POWRE grant for partial support. A. V. K. and G. V. U. were partially supported by INTAS grant 01-491 and RFBR grants 00-02-17253 and 00-01-00392.

REFERENCES

- Aly, J. J. 1980, A&A, 86, 192
Arons, J., & Lea, S. M. 1976a, ApJ, 207, 914
———. 1976b, ApJ, 210, 792
Bondi, H. 1952, MNRAS, 112, 195
Brio, M., & Wu, C. C. 1984, J. Comput. Phys., 75, 400
Camenzind, M. 1990, Rev. Mod. Astron., 3, 234
Ghosh, P., & Lamb, F. K. 1979, ApJ, 232, 259
Koldoba, A. V., Ustyugova, G. V., Lovelace, R. V. E., & Romanova, M. M. 2002, AJ, 123, 2019
Königl, A. 1991, ApJ, 370, L39
Lai, D. 1999, ApJ, 524, 1030
Li, J., & Wilson, G. 1999, ApJ, 527, 910
Lipunov, V. M. 1978a, Astronometriya Astrofiz., 36, 8
———. 1978b, AZh, 55, 1233
Lovelace, R. V. E., Romanova, M. M., & Bisnovatyi-Kogan, G. S. 1995, MNRAS, 275, 244
———. 1999, ApJ, 514, 368
Ostriker, E. C., & Shu, F. H. 1995, ApJ, 447, 813
Powell, K. G., Roe, P. L., Linde, T. J., Gombosi, T. I., & De Zeeuw, D. L. 1999, J. Comput. Phys., 154, 284
Romanova, M. M., Ustyugova, G. V., Koldoba, A. V., & Lovelace, R. V. E. 2002, ApJ, in press
Ronchi, C., Iacono, R., & Paolucci, P. S. 1996, J. Comput. Phys., 124, 93
Sadourny, R. 1972, Mon. Weather Rev., 100, 136
Sharleman, E. T. 1978, ApJ, 219, 617
Tanaka, T. 1994, J. Comput. Phys., 111, 381
Terquem, C., & Papaloizou, J. C. B. 2000, A&A, 360, 1031
Trümper, J., Kahabka, P., Ögelman, H., Pietsch, W., & Voges, W. 1986, ApJ, 300, L63